GYPSOPHILA SAPONINS ENHANCE THE CYTOTOXICITY OF ETOPOSIDE IN HD-MY-Z LYMPHOMA CELLS

Reneta Gevrenova[a], Maya M. Zaharieva[b], Alexander D. Kroumov[c], Laurence Voutquenne-Nazabadioko[d], Dimitrina Zheleva-Dimitrova[a], Vessela Balabanova[a], Hristo M. Hajdenski[b], Spiro Konstantinov[e]

[a]Department of Pharmacognosy, Faculty of Pharmacy, Medical University of Sofia, 2 Dunav St., 1000 Sofia, Bulgaria

[b]Department of Infectious Microbiology, The Stephan Angeloff Institute of Microbiology, Bulgarian Academy of Sciences, 26 Akad. G. Bonchev Str., 1113 Sofia, Bulgaria

[c]Department of Applied Microbiology, The Stephan Angeloff Institute of Microbiology, Bulgarian Academy of Sciences, 26 Akad. G. Bonchev Str., 1113 Sofia, Bulgaria

[d]Université de Reims Champagne Ardenne, CNRS, ICMR UMR 7312, 51097 Reims, France

[e]Department of Pharmacology, Pharmacotherapy and Toxicology, Faculty of Pharmacy, Medical University of Sofia, 2 Dunav St., 1000 Sofia, Bulgaria

*Corresponding author: Reneta Gevrenova, Department of Pharmacognosy, Faculty of Pharmacy, Medical University, 2 Dunav St., 1000 Sofia, Bulgaria

Tel.: +359 2 9236531; fax: +359 2 9879874.

E-mail address: rgevrenova@gmail.com; rgevrenova@pharmfac.mu-sofia.bg

Abstract

Glucuronide **O**leanane-type **T**riterpenoid **C**arboxylic **A**cid 3,28-**B**idesmosides (GOTCAB) are accumulated in *Gypsophila* L. roots. In the study we aimed at investigating the possible synergistic effects of *Gypsophila trichotoma* GOTCABs and cytostatic etoposide towards the Hodgkin lymphoma cell line HD-MY-Z. The combination effects with etoposide were evaluated using the symbolic mathematical software MAPLE. Liquid chromatography-mass spectrometry allowed the identification or tentative assignment of 28 core GOTCAB structures together with 6 monodesmosides in the root extract. Tested gypsogenin-based saponins possessed C-28 ester-bonded chain substituted with acetyl, *cis*/*trans* methoxycinnamoyl and both acetyl and sulphate groups. No cytotoxic effect was observed up to 20 µg/mL on normal mice fibroblasts (CCL-1 cell line) and lymphoma cells. Etoposide alone exerted IC_{50} 93 µg/mL. In the presence of acetylated saponins (20 µg/mL), a strong synergism (Fa=0.8, CI=0.1) was observed with IC_{50} 11 µg/mL. The combination induced apoptosis witnessed by caspase activation, elevated levels of cytosolic mono- and oligonucleosomes, and nuclear fragmentation together with discernible increase in ROS generation. The results emphasize the arabinose in the C-3 chain and acetylation pattern of the C-28 chain of the saponins as important structural features for cytotoxicity enhancing activity. Triterpenoid saponins are a valuable tool to improve the efficacy of cytostatics.

Keywords: GOTCAB saponins; *Gypsophila trichotoma*; etoposide; synergism; apoptosis; ROS

Highlights:

- 28 GOTCABs and 6 monodesmosides were characterized in *Gypsophila trichotoma* roots
- Synergistic effect of etoposide with 9 GOTCABs was tested on HD-MY-Z cell line
- Non-constant combination ratio etoposide/acetylated GOTCABs gave a strong synergism

- The combination induced apoptosis and interfered with the generation of ROS
- The enhancer possesses an arabinose in C-3 chain and acetylated C-28 ester chain

1. Introduction

Glucuronide **O**leanane-type **T**riterpenoid **C**arboxylic **A**cid 3, 28-**B**idesmosides (GOTCAB) saponins are among the highest glycosylated triterpenoid saponins (Henry, 2005). They are widespread in the advanced taxonomic groups Caryophyllidae, Rosidae and Asteridae (Henry, 2005; Cheikh-Ali et al., 2019). Structurally, GOTCABs contain a sapogenin with a characteristic aldehyde and carboxylic group linked at C-4 and C-28, respectively in the triterpenoid backbone. COTCABs contain two oligosaccharide chains attached at C-3 via glycosidic bond through glucuronic acid and ester-bonded chain at C-28 of the sapogenin. In the past 10 years a variety of GOTCABs were characterized from roots of wild and cultivated *Gypsophila* L. (Caryophyllaceae) species (Weng et al., 2010, Yao et al., 2010; Chen et al., 2011; Arslan et al. 2013; Voutquenne-Nazabadioko et al., 2013; Pertuit et al., 2014; Gevrenova et al., 2018a, b; 2019). The most commonly occurring sapogenins are gypsogenin and quillaic acid (Bottger and Melzig, 2010; Cheikh-Ali et al., 2019; Gevrenova et al., 2019). Recently, a new liquid chromatography – high resolution Orbitrap (LC-HRMS) acquisition strategy for the GOTCAB recognition was developed and the possible fragmentation pathways of a variety of saponins were proposed (Gevrenova et al., 2018a, b). The previous studies of *Gypsophila trichotoma* Wend. roots resulted in identification or tentative elucidation of more than 20 GOTCABs forming between two and four isobaric and positional isomers (Gevrenova et al., 2006; Voutqenne-Nazabadioko et al., 2013; Gevrenova et al., 2018a). The presence of sulfate or both sulfate and acetyl/methoxycinnamoyl group(s), as well as amino acid arginin in the ester-bonded chain is a structural feature of the *G. trichotoma* saponins. Apoptosis inducing activity of the *G. trichotoma*

root extract in monocytes/macrophages cell lines was witnessed by caspase-3 activation (Gevrenova et al., 2014). The synergistic cytotoxicity of nine newly isolated *G. trichotoma* GOTCABs in combination with type I ribosome-inactivating protein (RIP-I) saporin from *Saponaria officinalis* was tested on human breast cancer cell line 25 MDAMB-231 and a quantitative structure-activity relationship was derived (Gevrenova et al., 2015). The presence of a terminal xylose unit (not arabinose) in the branched C-3 trisaccharide is essential for the synergistic activity together with the acetyl group attached to the glucose residue in the ester-bonded tetrasaccharide. In addition, the aminoacyl *G. trichotoma* GOTCAB showed synergistic effect enhancing the cytotoxicity of saporin in HER14 cells (Voutqenne-Nazabadioko et al., 2013). In recent studies, the synergistic enhancement of the RIP I cytotoxicity by a variety of *Gypsophila* GOTCABs in *in vitro* and *in vivo* models was demonstrated (Bachran et al., 2008, 2009; Gilabert-Orol et al., 2013; Arslan et al., 2013; Fuchs et al., 2017). Moreover, Bottger et al., (2013) have defined a concept of the ideal saponin enhancer consisting of oleanane-type backbone, preferably gypsogenin and quillaic acid, a C-3 branched trisaccharide (glucuronic acid, galactose, xylose) and a partially esterified C-28 ester-bonded tetrasaccharide.

Another promising antitumor strategy is provided by the saponins' ability to enhance the conventional chemotherapeutics cytotoxicity (Sarkar and Li, 2006; Koczurkiewicz et al., 2015). Evidence came from the synergistically enhanced antitumor effect of combined saponins with chemotherapy by apoptotic pathway activation in human carcinogenesis models. Thus, ginsenoside R3 from *Panax ginseng* enhanced the effects of capecitabine and docetaxel in models of breast and prostate cancer, respectively (Zhang et al., 2008; Kim et al., 2010), while panaxadiol applied in combination with irinotecan induced caspase 3/9-dependent apoptosis in cancer intestinal cells (Du et al., 2012). It has been shown that saikosaponins sensitize cancer cells to the effects of cisplatin in Siha cells (normally resistant to cisplatin) (Wang et al., 2010).

Triterpenoid monodesmoside cyclamin synergistically enhanced the cytotoxicity of three chemotherapeutic drugs: 5-fluorouracil, cisplatin and epirubicinin human liver cancer cells (Li et al., 2014).

Based on all these studies, we aimed at investigating the enhancing activity of *G. trichotoma* GOTCABs in combination with the semisynthetic podophyllotoxin derivate etoposide (ETP) which claims to be a new contribution to the pharmacological characterization of the GOTCAB saponins as cytotoxicity enhancers. ETP exerts cytotoxicity by inhibiting the enzyme topoisomerase IIα/β inhibitor and thereby inducing DNA strand breaks and production of free radicals (Montecucco et al., 2015), and shows activity in both solid tumors and haematological malignancies by high-risk patients. However, a serious disadvantage in its clinical application is the presence of severe side effects on normal tissues and especially the high frequency development of secondary neoplasms (Montecucco et al., 2015, Shin et al., 2016). In this regard, a decrease of its dose through plausible combinations with cytotoxicity enhancers such as saponins would represent an effective way to ameliorate its genotoxic side effects, especially if there is a possibility to include the synergistic combination in formulations targeting preferably tumor cells (Kapoor and Singla, 2015; Koszurkewicz et al. 2016; Fuchs et al., 2017). As cell model system for our investigation we chose the Hodgkin lymphoma (HL) cell line HD-MY-Z considering the fact that etoposide is usually included in the therapeutic schemas for treatment of HL in combination with antibodies or cytostatics (Allen et al., 2017). This cell line was used as representative model for HL in several reports (Colleoni et al., 2002; Diaz, et al., 2011). In the present istudy, the pro-apoptotic effects of the combinations of ETP with GOTCAB saponins were also studied. In addition, in-depth characterization of the saponins in *G. trichotoma* root extract was performed by LC-HRMS.

2. Materials and methods

2.1. Plant material and G. trichotoma root extract

G. trichotoma roots were harvested in August 2004 from the Black Sea coast (Kavarna region) (43°25'60" N – 28°19'60" E) in Bulgaria and were identified by one of us (RG). Voucher specimen of plant material was deposed in the Herbarium of the Faculty of Pharmacy of Nancy, Universite de Lorraine, France (HP101). Air-dried powdered roots of the plant were extracted by sonication as previously described to yield lyophilized extract (Gt) (Gevrenova et al., 2014). The latter was dissolved in methanol (1 mg/mL), the solution was filtered through a 0.45 µm syringe filter disc (Polypure II, Alltech, Lokeren, Belgium) and subjected to UHPLC-HRMS.

2.2. Dataset of saponins and sample preparation

Nine GOTCAB saponins, previously isolated from *Gypsophila trichotoma* roots, were used for the combined cytotoxicity study with etoposide. Saponins were characterized on the basis of extensive NMR analysis (^{1}H, ^{13}C NMR, COSY, HSQC, HMBC, TOCSY, HSQC-TOCSY, ROESY), completed by HR-ESI-MS and ESI-MS^{n} analyses (Voutquenne-Nazabadioko et al., 2013). The structures of the saponin references are given in Fig. 1. The purities of saponins were over 90%, determined by LC-HRMS analyses. The extract Gt and each studied saponin was dissolved in DMSO at concentration 1mg/mL giving the stock solutions which were than filtered through a 0.22 µm filter (Millipore, MA) and stored at 4ºC until use. For the cell viability assays, the saponin stock solutions were diluted at 20 µg/mL, 10 µg/mL, 5 µg/mL; while Gt solution was diluted at the range of 100-0.01 µg/mL.

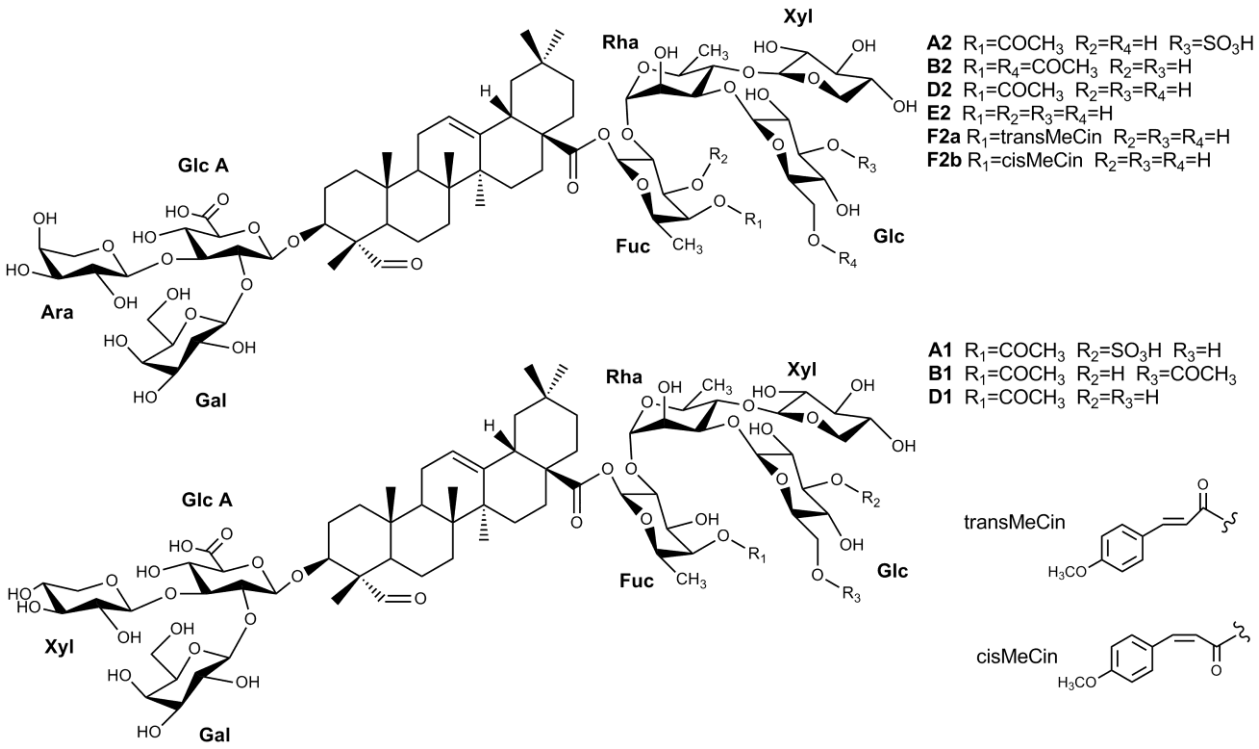

Fig. 1 Structures of the studied GOTCAB saponins from *G. trichotoma*

2.3. UHPLC-HRMS analysis and data processing

High resolution MS data of saponins were acquired on a Q-Exactive heated electrospray ionization (H-ESI)-high resolution mass spectrometer (Thermo Fisher Scientific, Waltham, MA, USA) connected to an UHPLC system equipped with an Accela autosampler and Accela quaternary UHPLC pump. The H-ESI source parameters were set as follows: 250ºC HESI vaporizer temperature, spray voltage at 3kV, ion transfer tube temperature at 300ºC, sheath gas pressure 35psi, auxiliary gas flow 10 (arbitrary units). The mass spectrometer was operated in negative ionization mode at a resolution 35000 FWHM (MS) and 17500 FWHM (MS/MS). Data were acquired over the mass range of *m/z* 400-2500 in Full MS-ddMS^2/Top 5 scan type, 80 msec maximal trap filling time, 4 *m/z* quadrupole isolation window of precursor ions, loop count 5, MSX count 1 (Gevrenova et al., 2018b). In stepped higher energy collision-induced dissociation

(hcd), two steps fragmentation on the precursor ions was proceed: 25 - (25 × 40%) and 25 + (25 × 40%). The chromatographic separation was carried out on Kinetex C18 (150 x 3 mm, 2.6 µm) (Phenomenex, USA). A binary gradient elution was performed at a flow rate 250 µL/min. The mobile phase A consisted of acetonitrile/0.08% formic acid in water 5:95 (v/v) and the mobile phase B - acetonitrile/0.08% formic acid in water 97:3 (v/v). The gradient program was as follows: 0-0.5 min, 100% A; 0.5-50 min, 100%A→100%B; 50-60 min, 100% B; 60-61 min, 100%B→100%A and the column was equilibrated for 5 min. The oven temperature was set at 40ºC. The injection volume was 1 µL. Data were processed using Xcalibur 3.0 ® (Thermo Scientific Co, USA) instrument control/data handling software.

2.4. Cell culturing

The antineoplastic activity of etoposide (ETP), *Gypsophila trichotoma* extract (Gt), saponins and combinations was evaluated on the Hodgkin lymphoma cell line HD-MY-Z (ACC-346, DSMZ, Braunschweig, Germany). The cells were maintained under sterile conditions (Laminar Airflow Bio II Advance, Telstar, Spain) in RPMI-1640 (#RPMI-HA, Capricorn®, Germany) supplemented with 10% FBS ((#FBS-HI-12A, Capricorn®, Germany) and 2 mM L-Glutamine (#G7513, Sigma® Life Science, Germany). They were incubated at 37 °C, 5% CO_2 and maximal humidity (Panasonic CO_2 incubator, #MCO-18AC-PE, Japan) and sub-cultured twice a week by splitting 1:4. The cytotoxicity of the saponins was evaluated on mouse fibsroblasts (NCTC clone 929: CCL 1, American Type Culture Collection [ATCC], Manassas, VA, USA), cultured in MEM (#MEM-A, Capricorn®, Germany) supplemented with 10 % Horse serum (#HOS-1A, Capricorn®, Germany).

2.5. Cell viability assay

The *in vitro* cytotoxicity of ETP, Gt extract and GOTCAB saponins was evaluated according to ISO 10993-5-2009 Annex C (ISO 10993-5:2009, 2017) which is based on the MTT reduction

assay (Mosmann, 1983). Briefly, cells were seeded in 96-well plates in starting density of $0.3x10^6$ cells/mL and incubated for 24 hours until entering the *log*-phase of the growth curve. Thereafter, they were exposed for 72 h to ETP or combinations between ETP (22.05 – 353.4 µg/mL, twofold serial dilutions) and GOTCAB saponins (5, 10 or 20 µg/mL). All experiments were performed in triplicate, wherein every sample was repeated four times. Cell viability was determined with the MTT dye in final concentration of 0.05 mg/mL after 2 h of incubation at 37°C. The formazan crystals were dissolved in isopropyl alcohol containing 5% HCOOH. The absorbance was measured at λ=550 nm (reference filter 690 nm) against a blank solution (culture medium, MTT and organic solvent) using an Absorbance Microplate Reader (#EL-800, Bio-Tek Instruments Inc., USA).

2.6. Determination of reactive oxygen species

The generation of reactive oxygen species (ROS) was measured using the commercially available Fluorometric Intracellular Ros Kit (#MAK143, Sigma® Life Science, Germany). The protocol of the manufacturer was followed by performing the experiment. Cells were seeded at density of $0.05x10^6$ cells/well and incubated for 24 hours prior treatment. The samples were incubated 6 hours with ETP or the respective combinations with GOTCAB saponins and the fluorimetric reaction product proportional to the amount of ROS present was measured at λ_{ex} = 490/ λ_{em}= 520 nm (Bio-Tek Instruments Inc., USA).

2.7. Homogenous caspases assay

The caspase activity in HD-MY-Z cells treated for 6 h with etoposide and combinations thereof with GOTCAB saponins was measured using a commercial kit of Roche (Sigma-Aldrich, #03 005 372 001) for quantitative fluorimetric evaluation of activated caspases 2, 3, 6, 7, 8, 9 and 10. The test was performed following the manufacturer's instructions (https://www.sigmaaldrich.com/content/dam/sigma-

aldrich/docs/Roche/Bulletin/1/caspassyrobul.pdf). Briefly, cells were seeded in a 96-well black plate with clear bottom, cultured for 24 h and exposed for 6 h to ETP or the test combinations. Thereafter, they were incubated in a lysis buffer containing caspase substrate. The fluorescence of the product was measured with an exication filter 490 nm and emission filter 520 nm (Bio-Tek Instruments Inc., USA).

2.8. Measurement of cytosolic mono- and oligonuclesomes

The quantitative *in vitro* determination of cytoplasmic histone-associated DNA fragments (mono- and oligonucleosomes) was done using a photometric enzyme immunoassay (#11 544 675 001, Roche Applied Science, Germany). Briefly, HD-MY-Z cells were seeded at density of $0.3x10^6$ cells/mL, incubated for 24 hours and treated with 22.02 µg/mL ETP or combinations between this concentration of ETP and 20µg/mL GOTCABS saponins B2 or D2. After 48 hours of exposure to the compounds, cells were counted and the protocol of the manufacturer was followed by performing the immunoassay. The signal was measured at λ=405 nm (490 reference wavelength) against a substrate solution blank.

2.9. Hoechst staining

DNA fragmentation was visualized by staining live cells with Hoechst 33342 (#14533, Sigma® Life Science, Germany) solution (100 µg/mL final concentration) for 30 min (Chazotte, 2016). Samples were observed on Nikon Eclipse Ti-U CLSM using 20× plan apochromatic objective. The EZ-C1 software was used for image acquisition.

2.10. Calculations of combination index in non-constant ratio of drugs

The median-effect principle (MEP) first formulated by Chou (1976) is widely applied in medicine and pharmacokinetic studies. The inhibition effect can be modeled with the equation based on the mass-action law as follows:

$$F_a/F_u=(Dose/D_m)^m \quad (1)$$

where F_a stands for affected fraction; F_u stands for unaffected fraction $(1\text{-}F_a)=F_u$; *Dose* stands for a dose of drug; *Dm* stands for a dose giving median-effect i.e. $Dm=IC_{50}$ (in our case); *m* is a slope of median-effect plot which means the shape of the dose-effect curve. For $m=1$ the curve is hyperbolic; for $m>1$ sigmoidal; for $m<1$ negative (flat) sigmoidal.

To accurately determine the values of "$Dm=IC_{50}$" and "*m*" we have been using nonlinear identification procedure coded in software of symbolic mathematics MAPLE®. On the basis of model simulation, we were being able to determine the value of *Dose* for every given F_a and vice versa. This approach differs from the linear one used by Chou and Martin in CompuSyn software. We analyzed this difference in details elsewhere (Zaharieva et al., 2018). Further, having values of "$Dm=IC_{50}$" and "*m*" we followed a step by step procedure to calculate the drug-drug interaction in predetermined concentrations interval. Hence, the combination index (CI) values for their non-constant ratio were calculated. More details about the theory and simulation of synergism and antagonism can be found elsewhere (Chou, 2006). In our case of non-constant ratio, the formula for calculation of CI value can be written as follows:

$$CI = \frac{(D_1)}{(D_x)_1} + \frac{(D_2)}{(D_x)_2} = \frac{(D)_{1,2}[\frac{P}{P+Q}]}{(D_m)_1[\frac{fa}{(1-fa)}]^{1/m_1}} + \frac{(D)_{1,2}[\frac{Q}{P+Q}]}{(D_m)_2[\frac{fa}{(1-fa)}]^{1/m_2}} \quad (2)$$

where CI <1, CI = 1, and CI > 1 indicate synergism, additive effect, and antagonism, respectively. In the denominator, (D_x) is for D_1"alone" that inhibits a system x%, and $(D_x)_2$ is for D_2"alone" that inhibits a system x%. The $(D_x)_1$ and $(D_x)_2$ values can be calculated from eq. 1. In the numerators, $(D)_1$ and $(D)_2$ "in combination" also inhibit x%. If the sum of these two fractional

terms in eq. 2 is equal to 1, additive effect is observed. If the CI value is smaller than 1, synergism is indicated, and if the CI value is greater than 1, antagonism occurred. A plot of CI on the y-axis as a function of effect levels (fa) on the x-axis is called Fa-CI plot which is well known in the literature. It should be noted that the extreme end of the CI values for synergism is from 0 to 1 and for antagonism is from 1 to infinity. Therefore, substituting, the "m" and "D_m" parameters, combination ratio P/Q into the corresponding equations given above, and setting Fa=0.01-0.99, the CI values at all effect levels can be simulated as Fa-CI table or Fa-CI Plot. Our default setting for calculation was Fa=0.5.

2.11. Statistics

The GraphPad Prism software (version 6.0.0 for Windows, San Diego, California USA, www.graphpad.com) was applied for preparation of the column graphs and the statistical analysis of the data based on Two-way ANOVA, whereby correction for multiple comparisons was performed with the Tukey test.

3. Results

3.1. In-depth characterization of saponins from G. trichotoma root extract

The non-targeted methabolic profiling of *G. trichotoma* methanol-aqueous extract was carried out by previously developed UHPLC-ESI/HRMS platform (Gevrenova et al., 2018b). The total ion chromatogram (TIC) and Full scan MS spectrum are depicted in Fig. S1. An acquisition strategy for structure elucidation of GOTCAB saponins (**G**lucuronide **O**leanane-type **T**riterpenoid **C**arboxylic **A**cid 3,28-*O*-**B**idesmosides) was applied (Gevrenova et al., 2018b). Herein, the negative mode collision-induced dissociations of 34 core structures were analyzed to outline the characteristic fragmentation pathways of the assayed saponins (Table S1, suppl. material). Our approach for saponin structural elucidation was based on the diagnostic fragment ions for different types of saponins in wild and cultivated *Gypsophila* species, and saponin references

(Gevrenova et al., 2018a,b; Gevrenova et al., 2019). Main criteria in the peak annotation are high accuracy MS and dd-MS^2 data, elemental composition, isotopic peak profiles, and database searching in an in-house library of GOTCABs. Sequential losses of the α-chain (C-28 ester-boned chain) and β-chain (C-3 glycosidic chain) gave fragment ions corresponding to the sapogenins involving *m/z* 469.332 $[C_{30}H_{45}O_4]^-$ for gypsogenin (G), *m/z* 485.327 $[C_{30}H_{45}O_4]^-$ for quillaic/gypsogenic acid (QA/GA) $[C_{30}H_{45}O_5]^-$and *m/z* 455.353 $[C_{30}H_{47}O_3]^-$ for oleanolic acid (OA) (Gevrenova et al., 2018b). Afterwards, due to both forms of decarboxylation, prominent fragment ions were observed at *m/z* 421.311 $[(QA-H)-HCO_2H-H_2O]^-$and *m/z* 405.316 $[(QA-H)-CO_2-2H_2O]^-$, while gypsogenic acid was deduced from the transition 485.327→423.326 $[(GA-H)- CO_2-H_2O]^-$ supported by *m/z* 405 (Table S1). Gypsogenin afforded low abundant ions at *m/z* 451.322 $[(G-H)-H_2O]^-$and 423.327 $[(G-H)-HCO_2H]^-$. The neutral mass losses of 162.053, 146.058, 132.042 and 176.033 were consistent with hexose (glucose/galactose), deoxyhexose (rhamnose/fructose), pentose (arabinose/xylose) and hexuronic acid. Consistent with the previous studies (Gevrenova et al., 2018b, 2019), GOTCAB fragmentation pattern involved a loss of α-chain at *m/z* 939.460 (G-derivatives), *m/z* 955.754 (QA/GA-derivatives) and 925.480 OA-derivatives) supported by the abundant fragment ions at *m/z* 565.354, 581.348 and 551.374 $[(M-H)-\alpha\text{ chain-Pent-Hex-}2H_2O\text{-}CO_2]^-$, respectively. Exemplified by **8**, the fragmentation pathway of GOTCABs gave a series of fragment ions in the low-mass region (*m/z* 100-400) in the dd-MS^2 spectrum indicative of the β-chain composition. The ions at *m/z* 319.067 (exact mass) $[(\beta\text{-chain-}H)-Pent-H_2O]^-$, *m/z* 289.057 $[(\beta\text{-chain-}H)-Hex-H_2O]^-$ and *m/z* 139.004 $[(\beta\text{-chain-}H)-Pen-Hex-2H_2O]^-$ together with *m/z* 807.420 $[(M-H)-\alpha\text{-chain-Pent}]^-$ and *m/z* 759.400 $[(M-H)-\alpha\text{-chain-Hex-}H_2O]^-$suggested both a branched β-chain and *O*-glycosylation of hexuronic acid (Table S1). The internal cleavages of the latter $^{0,2}A_{0\beta}$ (-134) and $^{4,5}A_{0\beta}$ (-58) resulted in the fragment ions at *m/z* 551.337 and 495.344, respectively. Moreover, the more abundant ion at *m/z* 759.397 (10.5%) was

informative of the hexose (1→2) linkage, while the (1→3) linked pentose was evidenced by the low abundant ions at *m/z* 745.417 (5.8%) and 727.409 (1.2%). Consistent with the earlier reports (Gevrenova et al., 2018b, 2019), except for **16** and **29**, the β-chain was identified as *O*-β-D-galactopyranosyl-(1→2)-[pentosyl-(1→3)]-β-D-glucuronopyranoside with variable pentose residue arabinose/xylose (Table S1). In addition to the previously reported 21 core GOTCAB structures, numerous minor saponins were tentatively identified including 5 monodesmosides and 16 bidesmosides (GOTCABs) (Table S1 and 1). The characteristic fragmentations $[M-H]^-$ →549.289 [3-*O*-sulfo-gypsogenin-H] and 565.284 [3-*O*-sulfo-gypsogenic acid-H] were used as diagnostic information to elucidate five 3-*O*-sulfated monodesmosides (Table S1). In line with the previously identified *Gypsophila* GOTCABs, five main types α-chains were evidenced: oligosaccharides (tri- to hexasacchride) (type I), α-chain substituted with sulfate group (type II), acetyl group(s) (type III), methoxycinnamoyl group (type IV), and both sulphate and acetyl/ methoxycinnamoyl groups (type V) (Table 1). Concerning type I saponins, five core structures are G-bidesmosides and 4 - QA-derivatives. **11** and **12** shared the same $[M-H]^-$ at *m/z* 1511.655 but QA-derivative (**11**) was deduced from the relevant fragment ions at *m/z* 955.455, 775.393, 485.3271 and 405.318, while G-based GOTCAB **12** was witnessed by the key fragments at *m/z* 939.460, 565.353, 469.332 and 423.326 (Table S1) (Gevrenova et al., 2018b). **16** was a typical type II saponin since a base peak corresponding to the α-chain together with the fragment ions at 579.124 $[^{1,3}X_{0\alpha}]^-$, 519.102 $[C_{1\alpha}]^-$, 503.108 $[Y_{2\alpha'}/^{3,4}X_{0\alpha}]^-$ were acquired in the MS/MS spectrum of $[M-H]^-$ at *m/z* 1443.574 (Table S1). The sulfate group is bonded to the hexose moiety witnessed by the ion at *m/z* 241.0015 $[^3X_{2\alpha}]$ seen previously in the saponin references spectra (Gevrenova et al., 2018a,b). Eight core structures from type III possessed varied monoacetylated (**18**, **20**, **22**, **23**) and diacetylated (**19**, **21**, **24**, **25**) α-chains supported by the fragment ions $[M-H-Ac]^-$ and $[M-H-AcOH]^-$ (Table S1).

Table 1. Tentative assignment and fragmentation pathway of saponins in *Gypsophila trichotoma* roots

N	Formula Exact mass of the saponins	Number of the separated isobaric isomers	Sapoge-nin	Tentative assignment of β-chain	Tentative assignment of α-chain	Species with related GOTCABs (literature data)	Reference
Monodesmosides							
1	$C_{48}H_{76}O_{22}S$ 1036.4549	2	G[a]	SO_3H	3Hex		
2	$C_{48}H_{76}O_{23}S$ 1052.4498	2	GA	SO_3H	3Hex		
3	$C_{53}H_{84}O_{26}S$ 1168.4972	2	G	SO_3H	3Hex, Pent		
4	$C_{54}H_{86}O_{27}S$ 1198.5077	3	G	SO_3H	4Hex		
5	$C_{54}H_{86}O_{28}S$ 1214.5026	3	GA	SO_3H	4Hex		
6	$C_{47}H_{72}O_{19}$ 940.4668	1	G	Pent, Hex, HexA[b]	-	*G. trichotoma*, *G. pacifica*	Nie et al., 2009; Yotova et al., 2012

Bidesmosides with C-28 oligosaccharide							
7	$C_{64}H_{100}O_{31}$ 1364.6249	2	G	Pent, Hex, HexA[b]	2dHex, Pent	*G. glomerata*	Gevrenova et al., 2018b
8	$C_{65}H_{102}O_{32}$ 1394.6354	2	G	Pent, Hex, HexA[b]	2dHex, Hex		
9	$C_{69}H_{110}O_{34}$ 1482.6878	1	OA	Pent, Hex, HexA[b]	2dHex, 2Pent	*G. glomerata*	Gevrenova et al., 2018b
10	$C_{69}H_{108}O_{35}$ 1496.6671	2	G	Pent, Hex, HexA[b]	2dHex, 2Pent	*G. oldhamiana* *G. glomerata*	Luo et al., 2008; Gevrenova et al., 2018b
11	$C_{69}H_{108}O_{36}$ 1512.6620	2	QA	Pent, Hex, HexA[b]	2dHex, 2Pent	*G. glomerata*	Gevrenova et al., 2018b
12	$C_{69}H_{108}O_{36}$ 1512.6620 isobar	1	G	Pent, Hex, HexA[b]	dHex, 2Pent, Hex	*G. glomerata*	Gevrenova et al., 2018b
13	$C_{70}H_{110}O_{36}$ 1526.6777	2	G	Pent, Hex, HexA[b]	2dHex, Pent, Hex[a]	*G. paniculata*, *G. oldhamiana*, *G.arrostii* var. *nebulosa* *G.trichotoma*, *G. glomerata*, *G. scorzonerifolia*, *G. pacifica*, *G. acutifolia*, *G. altissima*, *G. zhegualensis*	Frechet et al., 1991; Weng et al., 2010; Zhang *et al.*, 2013; Arslan et al., 2013; Voutquenne-Nazabadioko et al., 2013; Gevrenova et al., 2018a,b, 2019

14	$C_{70}H_{110}O_{37}$[b] 1542.6777	2	QA	Pent, Hex, HexA[b]	2dHex, Pent, Hex	*G. paniculata*, *G.arrostii* var. *nevulosa*, *G. pilulifera*, *G. glomerata*, *G. scorzonerifolia*, *G. pacifica*, *G. acutifolia*, *G. altissima*, *G. oldhamiana*, *G. zhegualensis*	Frechet et al., 1991; Weng et al., 2010; Yao et al., 2010; Arslan et al., 2013; Gevrenova et al., 2018b, 2019
15	$C_{80}H_{126}O_{45}$ 1806.7571	2	QA	Pent, Hex, HexA[b]	2dHex, 3Pent, Hex		
Bidesmosides with C-28 oligosaccharide substituted with sulfate group							
16	$C_{64}H_{100}O_{34}S$ 1444.5817	2	G	Pent, HexA	2dHex, Pent, Hex, SO_3H		
17	$C_{70}H_{110}O_{39}S$ 1606.6345	2	G	Pent, Hex, HexA[b]	2dHex, Pent, Hex, SO_3H	*G. trichotoma*, *G. glomerata*	Gevrenova et al., 2018a,b
Bidesmosides with C-28 oligosaccharide substituted with acetyl group(s)							
18	$C_{67}H_{104}O_{33}$ 1436.6460	2	G	Pent, Hex, HexA[b]	2dHex, Hex, Ac	*G. trichotoma*,	Gevrenova et al., 2018a
19	$C_{69}H_{106}O_{34}$ 1478.6565	2		Pent, Hex, HexA[b]	2dHex, Hex, 2Ac		
20	$C_{72}H_{112}O_{37}$	4	G	Pent, Hex,	2dHex, Pent, Hex,	*G. oldhamiana*,*G.trichotoma*,	Luo et al., 2008

	1568.6882			HexA[b]	Ac	*G. glomerata, G. paniculata, G. scorzonerifolia, G. pacifica, G. acutifolia, G. altissima, G. zhegualensis*	Voutquenne-Nazabadioko *et al.*, 2013; Gevrenova et al., 2018a,b, 2019
21	$C_{74}H_{114}O_{38}$ 1610.6988	2	G	Pent, Hex, HexA[b]	2dHex, Pent, Hex, 2Ac	*G.trichotoma, G. paniculata, G. scorzonerifolia, G. pacifica, G. acutifolia, G. altissima, G. oldhamiana, G. zhegualensis*	Voutquenne-Nazabadioko *et al.*, 2013; Gevrenova et al., 2018a, 2019
22	$C_{77}H_{120}O_{41}$ 1700.7305	3	G	Pent, Hex, HexA[b]	2dHex, 2Pent, Hex, Ac	*G. glomerata, G. paniculata, G. scorzonerifolia, G. pacifica, G. acutifolia, G. altissima, G. oldhamiana, G. zhegualensis*	Gevrenova et al., 2018b, 2019
23	$C_{77}H_{120}O_{41}$ 1700.7305 isobar	1	QA	Pent, Hex, HexA[b]	3dHex, 2Pent, Ac	*G. paniculata, G. pacifica, G. scorzonerifolia, G. acutifolia, G. altissima, G. oldhamiana, G. zhegualensis*	Gevrenova et al., 2019
24	$C_{79}H_{122}O_{43}$ 1742.7411	4	G	Pent, Hex, HexA[b]	2dHex, 2Pent, Hex, 2Ac	*G.trichotoma, G. paniculata, G. scorzonerifolia, G. pacifica, G. acutifolia, G. altissima, G. oldhamiana, G. zhegualensis*	Voutquenne-Nazabadioko *et al.*, 2013; Gevrenova et al., 2018a, 2019

25	$C_{80}H_{124}O_{43}$ 1772.7516	2	G	Pent, Hex, HexA[b]	2dHex, Pent, 2Hex, 2Ac		
Bidesmosides with C-28 oligosaccharide substituted with methoxycinnamoyl group							
26	$C_{80}H_{118}O_{38}$ 1686.7301	2	G	Pent, Hex, HexA[b]	2dHex, Pent, Hex, Mecin	*G.trichotoma, G. paniculata, G. scorzonerifolia, G. pacifica, G. acutifolia, G. altissima, G. oldhamiana, G. zhegualensis*	Voutquenne-Nazabadioko *et al.*, 2013; Gevrenova et al., 2019
27	$C_{85}H_{126}O_{42}$ 1818.7724	4	G	Pent, Hex, HexA[b]	2dHex, 2Pent, Hex, Mecin		
28	$C_{87}H_{128}O_{43}$ 1860.7829	4	G	Pent, Hex, HexA[b]	2dHex, 2Pent, Hex, Mecin, Ac	*G. paniculata, G. pacifica, G. scorzonerifolia, G. acutifolia, G. altissima, G. oldhamiana, G. zhegualensis*	Gevrenova et al., 2019
Bidesmosides with C-28 oligosaccharide substituted with both sulfate and acetyl/methoxycinnamoyl groups							
29	$C_{67}H_{104}O_{36}S$ 1516.6028	1	G	Hex, HexA	dHex(C4-Ac), dHex, Pent, Hex(SO_3H)		
30	$C_{72}H_{112}O_{40}S$ 1648.6451	1	G	Pent, Hex, HexA[b]	dHex(C3-Ac), dHex, Pent,	*G.trichotoma*	Voutquenne-Nazabadioko *et al.*, 2013

					Hex(SO_3H)		
31	$C_{72}H_{112}O_{40}S$ 1648.6451 isobar	2	G	Pent, Hex, HexA[b]	dHex(C4-Ac), dHex, Pent, Hex(SO_3H)	*G.trichotoma* *G. scorzonerifolia*	Voutquenne-Nazabadioko *et al.*, 2013; Gevrenova et al., 2019
32	$C_{74}H_{114}O_{41}S$ 1690.6556	2	G	Pent, Hex, HexA[b]	dHex(C4-Ac), dHex, Pent, Hex (Ac, SO_3H)	*G.trichotoma*	Gevrenova et al., 2018a
33	$C_{76}H_{118}O_{44}S$ 1766.6717	2	G	Pent, Hex, HexA[b]	dHex(C4- Mecin), dHex, Pent, Hex(SO_3H)	*G.trichotoma*	Gevrenova et al., 2018a
34	$C_{77}H_{120}O_{44}S$ 1780.6873	1	G	Pent, Hex, HexA[b]	dHex(C4-Ac), dHex, 2Pent, Hex(SO_3H)	*G.trichotoma*	Gevrenova et al., 2018a

[a]G, gypsogenin; GA, gypsogenic acid; QA, quillaic acid; OA, oleanolic acid; Pent, pentose; Hex, hexose; dHex, deoxyhexose; HexA, hexuronic acid; SO_3H, sulphate group; Ac, acetyl group; Mecin, methoxycinnamoyl group

[b]*O*-β-D-galactopyranosyl-(1→2)-[pentosyl-(1→3)]-β-D-glucuronopyranoside

By analogy with the fragmentation pattern of GOTCABs isolated from *G. trichotoma*, methoxycinnamoyl (**26**, **27**) and both acetyl and methoxycinnamoyl (**28**) groups were located, witnessed by the fragment ions at *m/z* 177.055 $[MeCinO]^-$, 145.029 $[MeCinO\text{-}CH_3OH]^-$ and 117.034 $[MeCinO\text{-}CH_3OH\text{-}CO]^-$ (**26**, type IV) (Table S1). Regarding the type V, in addition to the diagnostic ions for sulfated GOTCABs, the internal cleavages $^{3,4}A_{0\alpha}$ and $^{3,5}A_{0\alpha}$ indicated acetyl/methoxycinnamoyl group at C-4 dHex hydroxyl (**29**, **31**-**34**), while $^{0,2}X_{0\alpha}$ evidenced acetylation at C-3 (**30**) (Table S1). By comparative analysis of the fragmentation patterns, the modifications of the α-chain were primarily characterized to involve supplementary pentose unit in saponins with molecular mass 1496 and 1526 compared to 1364 and 1394, respectively (Table 1). Core structures with molecular mass1700, 1742, 1818 and 1860 could be associated with derivatives of 1496 with an additional hexose unit in the α-chain. Thus, 1700 and 1742 possessed monoacetylated and diacetylated α-chain, respectively, while methoxycinnamoyl residue was deduced in 1818 and both acetyl and methoxycinnamoyl groups were evidenced in 1860. Saponin 1780 is sulphated derivative of 1700. In the same way, mono- and diacetylated trisaccharide (1436 and 1478) and tetrasaccharide (1568 and 1610) were acquired by MS/MS spectra of the precursor ions. Fragmentation behaviour of 1772 was in agreement with that of 1610, except for the appearance of an additional hexose unit in the α-chain. In addition, sulfated derivatives of 1610 and 1526 were ascribed to 1690 and 1606, respectively. Gypsogenin- and quillaic acid-GOTCABs shared the same oligosaccharide chains in saponins with masses 1526 and 1542 (2dHex, Pent, Hex). Likewise, a similar α-chain was suggested in 1496 (G-GOTCAB), 1512 (QA-GOTCAB) and 1482 (OA-GOTCAB).

3.2. In vitro cytotoxicity of ETP and combinations with GOTCAB saponins

The crude *Gypsophila trichotoma* (Gt) extract was not cytotoxic to HD-MY-Z cells in concentrations between 0.01-10 µg/mL. Concentrations higher than 10 µg/mL diminished significantly the cell viability after 72 h of incubation (IC_{50}=78.64 µg/mL) (Fig. 2).

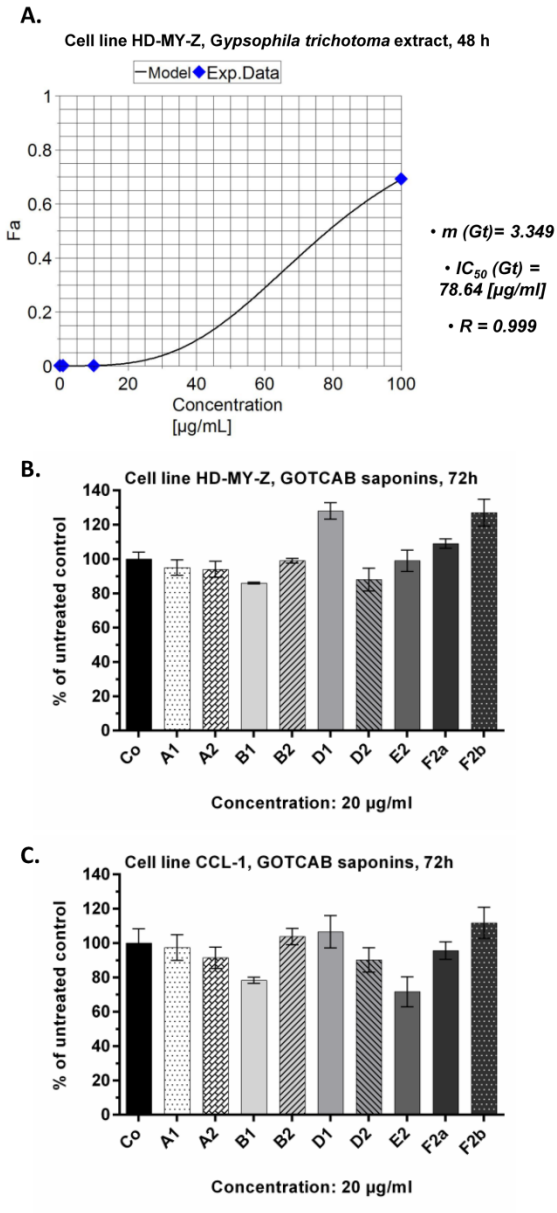

Figure 2. *In vitro* cytotoxicity of ETP and GOTCAB saponins in HD-MY-Z cells. **(A)** *In vitro* cytotoxicity of *G. trichotoma* extract (Gt) on HD-MY-Z cells; **(B)** *In vitro* cytotoxicity of

GOTCAB saponins on HD-MY-Z cells after 72h of treatment; **(C)** *In vitro* cytotoxicity of GOTCAB saponins on CCL-1 cells after 72h of treatment.

GOTCAB saponins were not cytotoxic for this cell line up to 20 µg/mL (the highest concentration used for the combinations) after 72 hours of treatment, except for B1 and D2 that slightly inhibited the cell viability by 14 and 12%, respectively (Fig. 2). Both effects could not be considered as cytototoxic because the values are significantly lower than 30 % (ISO 10993-5-2009). On the contrary, saponins D1, F2a and F2b stimulated significantly the cell proliferation by 28, 9 and 27%, respectively. The One-way ANOVA analysis of differences is given in Table S2. GOTCAB saponins did not exert significant cytotoxicity on a cell line of normal mice fibroblasts CCL-1 (Table S3) as compared to the untreated control except for saponins B1 and E2 which decreased the cell viability by 21.8 ± 1.7 % and 28.4 ± 8.7 %, respectively. The latter value is indicative for cytotoxic effect.

The *in vitro* cytotoxicity and combination effects of ETP and GOTCABs are presented in Table 2 and Figure 3. The strongest synergism was achieved by combining ETP with saponins B2, D2 and F2a (Fig. 3), whereas the other saponins led to different combinations effects varying from synergism to strong antagonism depending on the concentration of ETP used (Table 2). The IC_{50} value of the combination between ETP and 20 µg/mL D2 is approximately eighth fold lower than that of ETP alone. The other two saponins B2 and F2a diminished the IC_{50} value of ETP almost by half. All CI values in Figure 3 are indicative for slight to strong synergism (Chou, Martin, 2005).

Response surface analysis (RSA) shown in Figure 3A (See Fa=f(Conc.,m) and Fa =f(Conc., IC50)) demonstrated the predictive power of the model (eq.1) when the evaluated values of “m”

and “IC50” changed in the intervals determined by standard deviation of these two parameters. Therefore, a wide range of experimental data variation can successfully be described by application of the model. Note: In all cases, the calculated "R" correlation coefficient by MAPLE procedure was much better than that calculated by CompuSyn and GraphPad Prism software.

Table 2. Combination effects of ETP and GOTCAB saponins

Concentration of ETP [µg/mL]	**22.02**	**44.18**	**88.35**	**176.7**	**353.4**
Fa (ETP)	0.38±0.01	0.41±0.01	0.40±0.01	0.58±0.08	0.90±0.01
Fa (ETP+20 µg/mL A1)	0.06±0.01	0.08±0.02	0.23±0.06	0.86±0.004	0.84±0.01
CI value	7.99	11.11	5.38	***0.33***	***0.80***
Fa (ETP+20 µg/mL A2)	0.38±0.02	0.37±0.01	0.41±0.01	0.62±0.02	0.84±0.004
CI value	***0.62***	1.27	2.06	1.54	***0.81***
Fa (ETP+20 µg/mL B1)	0.23±0.01	0.25±0.01	0.26±0.02	0.85±0.01	0.81±0.002
CI value	1.49	2.5	4.57	***0.39***	1.04
Fa (ETP+20 µg/mL D1)	0.34±0.01	0.40±0.01	0.49±0.02	0.86±0.01	0.87±0.004
CI value	NaN	NaN	NaN	***0.33***	***0.60***
Fa (ETP+20 µg/mL E2)	0.48±0.01	0.49±0.04	0.53±0.03	0.84±0.02	0.88±0.01
CI value	***0.36***	***0.70***	1.16	***0.40***	***0.54***
Fa (ETP+20 µg/mL F2b)	0.14±0.03	0.18±0.02	0.23±0.03	0.39±0.05	0.82±0.01
CI value	NaN	NaN	NaN	NaN	0.94

Legend: **ETP** = etoposide; **A1, B1, D1, E2, F2a** – GOTCAB saponins; **Fa** = effect; **CI** = combination index; **NaN** = not a number; **CI ≤ 0.9** – synergism, **0.9 ≤ CI ≤ 1.1** – nearly additive, **CI ≥ 1.1** – antagonism.

A. ETP

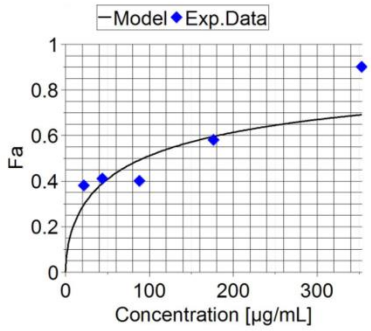

m (A)=0.602
IC_{50} (A)=93.35 [µg/mL]
R (A)=0.9328

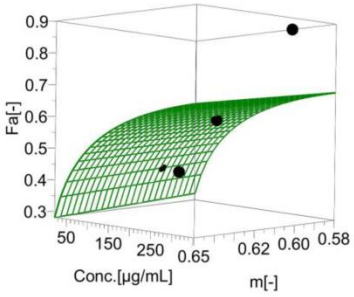

m (A)= 0.58 - 0.65
IC_{50} (A)=93.35 [µg/mL]
R (A)=0.9328

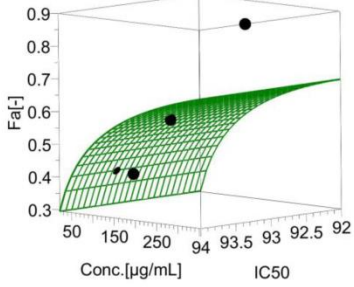

m (A)=0.602
IC_{50} (A)= 92.78 - 94.78 [µg/mL]
R (A)=0.9328

B. ETP + 20 µg/mL B2

m (AB)= 2.0
IC_{50} (AB)= 57.0 [µg/mL]
R (AB)= 0.942
CI [22.02*/20**]=0.32; Fa=0.61
CI [44.18/20]=0.42; Fa=0.71
CI [88.35/20]=0.50; Fa=0.68
CI [176.7/20]=0.55; Fa=0.85
CI [353.4/20]=0.58; Fa=0.84

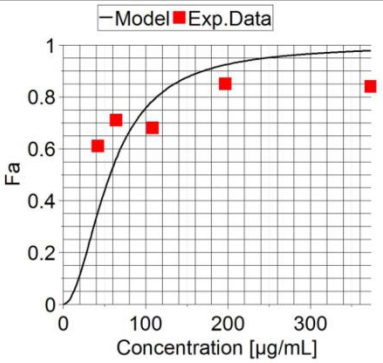

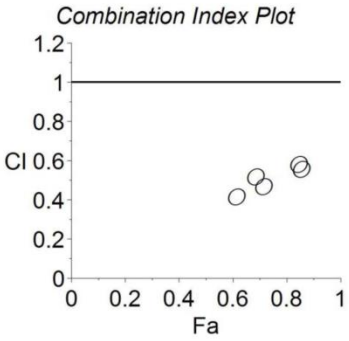

C. ETP + 20 µg/mL D2

m (AB)=1.16
IC_{50} (AB)= 11.5 [µg/mL]
R (AB)= 0.974
CI [22.02/20]=0.06; Fa=0.80
CI [44.18/20]=0.08; Fa=0.85
CI [88.35/20]=0.10; Fa=0.88
CI [176.7/20]=0.11; Fa=0.88
CI [353.4/20]=0.12; Fa=0.87

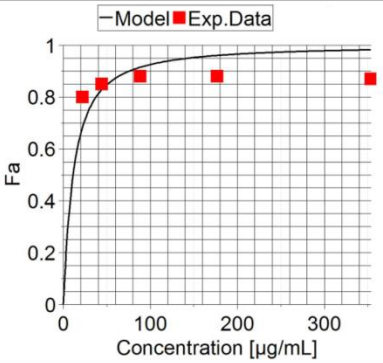

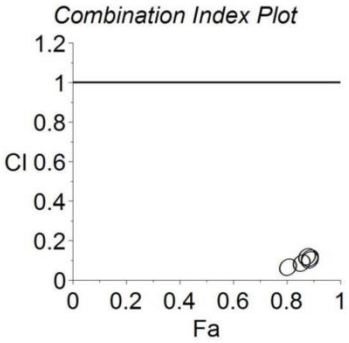

D. ETP + 20 µg/mL F2a

m (AB)= 1.053
IC_{50} (AB)= 57.0 [µg/mL]
R (AB)= 0.86
CI [22.02/20]=0.41; Fa=0.61
CI [44.18/20]=0.47; Fa=0.60
CI [88.35/20]=0.52; Fa=0.55
CI [176.7/20]=0.55; Fa=0.69
CI [353.4/20]=0.58; Fa=0.84

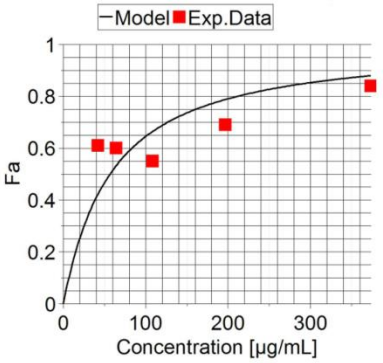

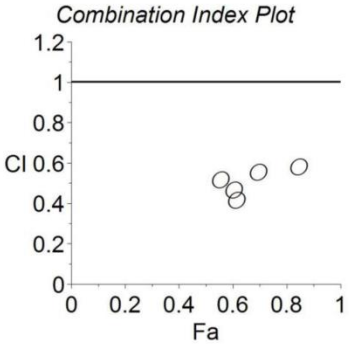

Figure 3. *In vitro* cytotoxicity of ETP and combinations between ETP and GOTCAB saponins. **(A)** *In vitro* cytotoxicity of ETP with response surface analysis; **(B)** *In vitro* cytotoxicity of combinations between ETP and 20 µg/ml saponin B2 with a Combination index plot; **(C)** *In vitro* cytotoxicity of combinations between ETP and 20 µg/ml saponin D2 with a Combination index plot; (**D**) *In vitro* cytotoxicity of combinations between ETP and 20 µg/ml saponin F2a with a Combination index plot; **Legend**: **ETP** = etoposide; **B2, D2, F2a** = GOTCAB saponins; **Fa** = effect; **m** = slop of median-effect plot; **IC_{50}** = concentration that inhibits the cell viability by 50%; **R** = correlation coefficient; **CI** = Combination Index; *****Concentration of ETP [µg/mL]; ******Concentration of saponin [µg/mL]; **CI ≤ 0.9** – synergism, **0.9 ≤ CI ≤ 1.1** – nearly additive, **CI ≥ 1.1** – antagonism.

3.3. Induction of ROS and apoptosis in HD-MY-Z cells after exposure to synergistic combinations between ETP and GOTCAB saponins

Tests for generation of ROS and induction of programmed cell death were conducted for the two combinations which exhibited the strongest synergistic inhibitory effect on the viability of HD-MY-Z cells. As visible from Fig. 4A, after 6 hours of incubation, there was a concentration-dependent increase in the amount of generated intracellular ROS, more pronounces for both combinations, and namely from 13% (22.02 µg/mL ETP + 20 µg/mL B2) and 19% (22.02 µg/mL ETP + 20 µg/mL D2) higher up to 52% (353.4 µg/mL ETP + 20 µg/mL B2) and 67% (353.4 µg/mL ETP + 20 µg/mL D2) higher than ETP alone. The two-way ANOVA analysis of the differences is given in Table S4.

Apoptosis induction was evaluated using three different methods: (1) activation of caspases; (2) accumulation of mono- and oligonucleosomes in the cellular cytosol and (3) visualization of

DNA fragmentation. Measurement of homogenous caspase activation showed a concentration-dependent increase in enzyme activity, most pronounced for combinations of ETP with B2 and D2 than ETP alone concerning ETP concentrations ≥ 44.18 µg/mL in combination with 20 µg/mL B2 or D2 (Fig. 4B, two-way ANOVA analysis, Table S5).

The quantitative analysis of the fraction of cytoplasmic histone-associated DNA fragments performed with 22.02 µg/ml ETP alone or in combinations with 20 µg/mL B2 or D2 after 48 h of treatment showed that the combinations led to accumulation of higher (13 and 25%, respectively) quantity of mono- and oligonucleosomes in the cellular cytosol than ETP alone (Fig. 4C). The One-way ANOVA analysis is presented in Table S6. In parallel, the qualitative microscopic observation of Hoechst stained samples revealed higher degree of DNA fragmentation as compared to the untreated control and ETP alone (Fig. 4D).

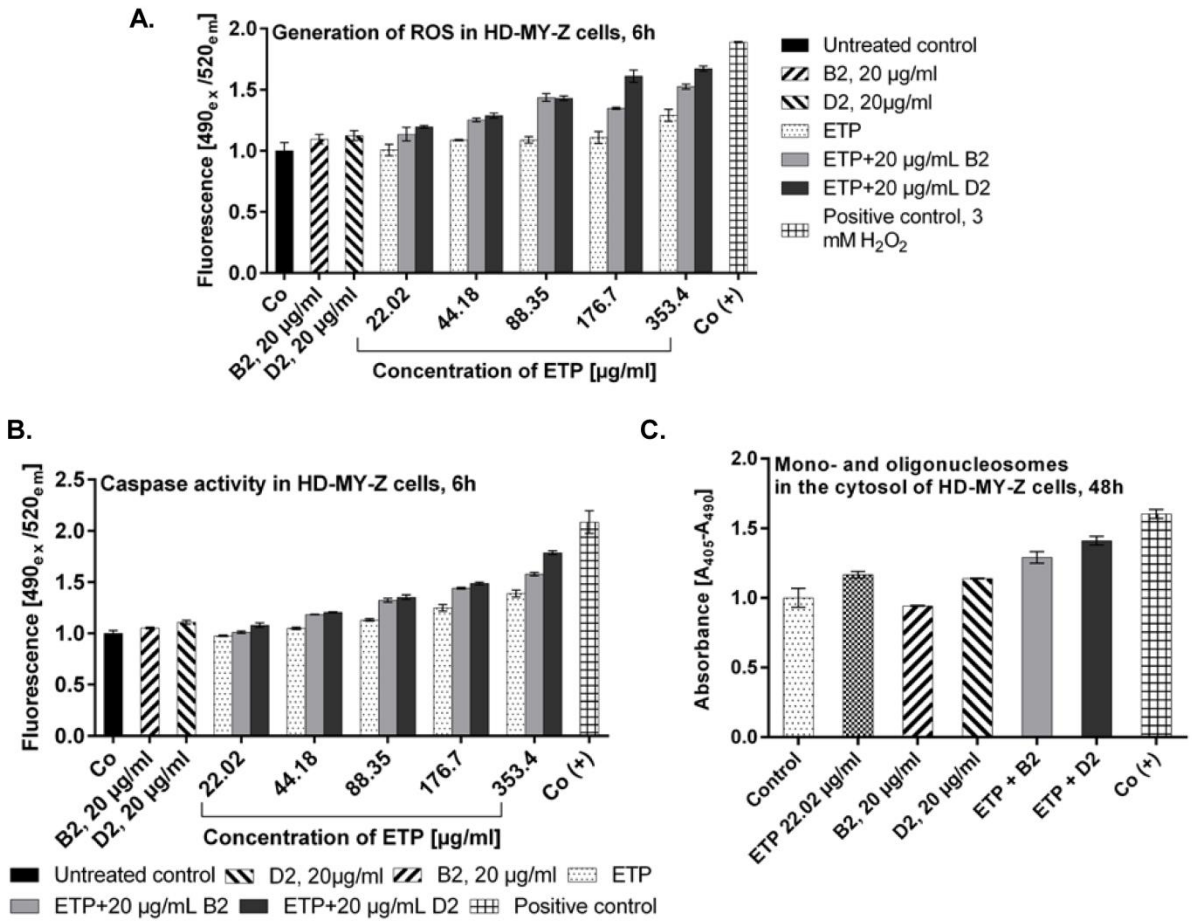
A.
Generation of ROS in HD-MY-Z cells, 6h
Fluorescence [490ex /520em]
2.0
1.5
1.0
0.5
0.0
Co
B2, 20 µg/ml
D2, 20 µg/ml
22.02
44.18
88.35
176.7
353.4
Co (+)
Concentration of ETP [µg/ml]
Untreated control
B2, 20 µg/ml
D2, 20µg/ml
ETP
ETP+20 µg/mL B2
ETP+20 µg/mL D2
Positive control, 3 mM H2O2
B.
Caspase activity in HD-MY-Z cells, 6h
Fluorescence [490ex /520em]
2.5
2.0
1.5
1.0
0.5
0.0
Co
B2, 20 µg/ml
D2, 20 µg/ml
22.02
44.18
88.35
176.7
353.4
Co (+)
Concentration of ETP [µg/ml]
Untreated control
D2, 20µg/ml
B2, 20 µg/ml
ETP
ETP+20 µg/mL B2
ETP+20 µg/mL D2
Positive control
C.
Mono- and oligonucleosomes in the cytosol of HD-MY-Z cells, 48h
Absorbance [A405-A490]
2.0
1.5
1.0
0.5
0.0
Control
ETP 22.02 µg/ml
B2, 20 µg/ml
D2, 20 µg/ml
ETP + B2
ETP + D2
Co (+)

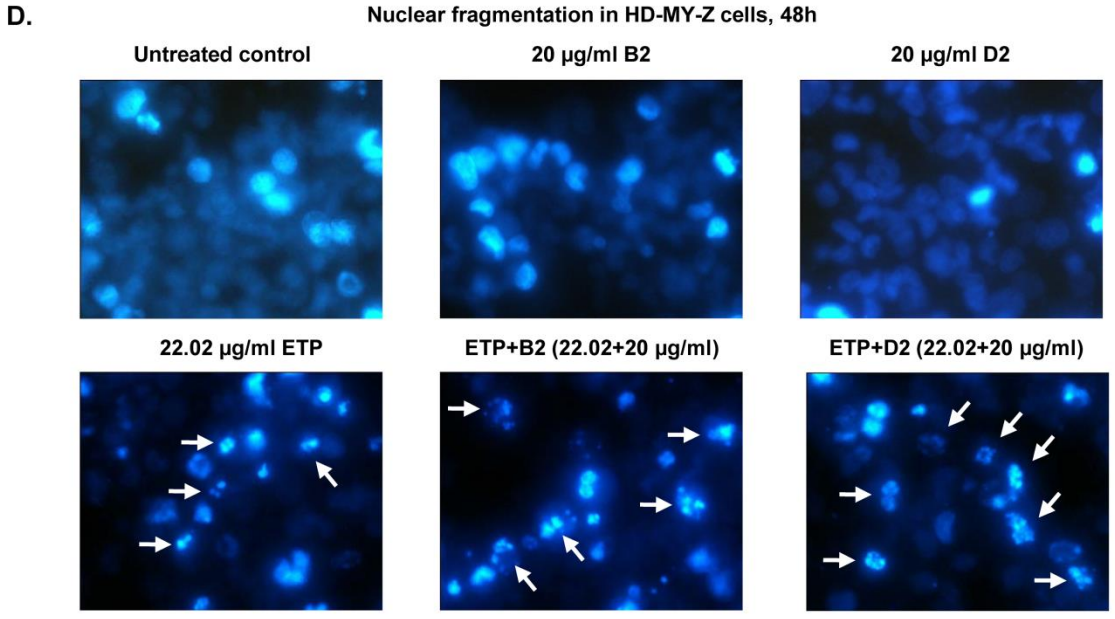
D.
Nuclear fragmentation in HD-MY-Z cells, 48h
Untreated control
20 µg/ml B2
20 µg/ml D2
22.02 µg/ml ETP
ETP+B2 (22.02+20 µg/ml)
ETP+D2 (22.02+20 µg/ml)

Figure 4. **(A)** Generation of free radicals in HD-MY-Z cells after 6 h of exposure to ETP and combinations between ETP and 20 µg/ml B2 or D2; **(B)** Caspase activation in HD-MY-Z cells after 6 h of exposure to ETP and combinations between ETP and 20 µg/ml B2 or D2, **(C)** Accumulation of mono- and oligonucleosomes in the cytosol of HD-MY-Z cells after48 h of exposure to ETP and combinations between ETP and 20 µg/ml B2 or D2; **(D)** DNA fragmentation in HD-MY-Z cells after 48 h of exposure to ETP and combinations between ETP and 20 µg/ml B2 or D2.

4. Discussion

In the current study, in-depth characterization of the saponin profiling of *G. trichotoma* roots was achieved by liquid chromatography – high resolution Orbitrap mass spectrometry acquisition platform. Altogether, a total of 27 core structures derived from gypsogenin, while 4 corresponded to the quillaic acid-based GOTCABs, 2 – to gypsogenic acid derivative and 1 – to oleanolic acid. Among the *G. trichotoma* mono- and bidesmosides 21 core structures appeared as isobaric pairs (Table 1). By analogy with data acquired on GOTCABs from *G. trichotoma*, the differentiation between the isobars could be associated with the terminal pentose residue in the β-chain (xylose/arabinose) (Voutquenne-Nazabadioko et al., 2013, Gevrenova et al., 2018b). In the majority of saponin pairs with acetylated/acylated α-chains the isobars arise from the substitution pattern of the oligosaccharides and possible migration of the functional groups between position 3 and 4 on the fucose residue and in reverse, as was seen previously in *G. trichotoma* and *Quillaia saponaria* Molina (Nord and Kenne, 2000, Voutquenne-Nazabadioko et al., 2013). In addition, *cis*- and *trans*-methoxycinnamoyl moieties caused the appearance of isobaric pairs (Chen et al., 2011; Voutquenne-Nazabadioko et al., 2013). Consequently, **20**, **22**, **24**, **27** and **28**

formed 3 and 4 isobars (Table 1). Sixteen minor GOTCAB core structures together with 5 3-*O*-sulfo-monodesmosides that were overlapped by the dominant ones are tentatively identified (Table 1). By searching in the in-house GOTCABs library, 15 core structures forming between 2 and 4 isomers have not been previously reported in *G. trichotoma*, whereas 6 are undescribed in the literature.

According to the published scientific data, triterpenoid saponins can inhibit the proliferation of tumor cells, reduce their invasive potential and exhibit anti-metastasis, anti-angiogenesis and reversal of multi-drug resistance effects (Bachran et al., 2008; Xu et al., 2016). Saponins from *Gypsophila* with an aldehyde group in the oleanane-type sapogenin exert tumor selective cytotoxic effects towards human cancer cell lines (Zhang et al., 2013; Arslan et al., 2013; Voutquenne-Nazabadioko et al., 2013). Most triterpenoid saponins exert their antitumor activity by apoptotic mechanisms (Koczurkiewicz et al., 2015), however, their potency as cytotoxicity enhancers is still quite unknown. There are recent reports on chemosensitizing effects of saponins showing synergistic activity with anticancer drugs (Fuchs et al., 2009; Koszurkewicz et al., 2015). A low cytotoxic level (1.25 μM) of cyclamin, a 13,28-epoxyoleanane type saponin from *Ardisia japonica*, synergistically enhanced the activity of 5-fluoruracil, cisplatin and epirubicin on the liver cancer Bel-7402 and Hep G2, but not non-neoplastic liver cells (Li et al., 2014). Co-administration of *Lysimachia ciliata* saponins (0.5 μM) from the aforementioned saponin type and mitoxantrone exerted synergistic cytostatic and proapoptotic effects (Koszurkewicz et al. 2016). Ginsenosides and saikosaponins sensitizes cancer cells to the effects of chemotherapeutic agents (Xu et al., 2016, Koszurkewicz et al. 2015). Indeed, ginsenoside Rg3 enhanced the anticancer effects when combined with cyclophosphamide, capecitabine, docetaxel, cisplatin, doxorubicine (Xu et al., 2016).

The mechanisms underlying the synergistic effects of saponins in combination with cytostatics or other antineoplastic compounds have been investigated in numerous studies. The permeabilizing effects of the oleanane-type saponins on the cell and lysosomal membranes have been revealed by (Gilabert-Oriol e al., 2013). Enhancement of the membrane permeability resulted in an enhanced cellular uptake of RIP I and anticancer drugs (Bachran et al., 2008; Fuchs et al., 2017). Bidesmosidic saponins are well known to interfere with the membrane-cholesterol. Moreover, the occurrence of glucuronic acid, galactose, arabinose support the complexion of the membrane-cholesterol (Gauthier et al., 2009). In addition, acetyl, methoxycinnamoyl and short fatty acid residues can augment the lipophilicity and further increase a saponin impact on the membranes. According to Bottger et al. (2013) differences in the repair mechanisms of endosomal/lysosomal and cytosolic membranes have also function for the synergistic cytotoxicity.

Based on all these investigations, the main goal of this part of our study was to find the most suitable *Gypsophila* GOTCAB saponin for synergistic combinations with the semisynthetic podophyllotoxin derivate ETP which would achieve cytotoxic effect with significantly lower ETP concentrations than the single drug application. Such combinations could be used in future investigations for development of targeted therapy with specific formulations targeting preferably malignant cells. Following our hypothesis, we showed for the first time that combination treatment of not or low cytotoxic concentrations of *Gypsophila* GOTCAB saponins with ETP exerted a synergistic cytotoxic effect in the treated HL cell line. For our investigation we selected a HL cell line (HD-MY-Z) which was characterized by significantly higher IC_{50} value than a panel of B lymphoma cell lines described in the literature (Devin et al., 2017). In this study, the most prominent enhancers D2, B2 and F2a (20 µg/mL) were selected based on the IC_{50} and CI values of the combinations tested. All three saponins did not alter the viability of the

normal cell line (CCL-1) tested up to concentration of 20 µg/ml. In the combinations, they were applied in this low non-toxic concentration which was not expected according to published data for other saponins from the same or different type (Bottger et al., 2013; Koczurkiewicz et al., 2016; Li et al., 2014) to exert cytotoxic effect or to interfere with induction of apoptosis and, respectively, with the mode of action of ETP. The combined treatment with D2 turned out to be the most potent and resulted in discernible decrease in IC_{50} of ETP by eighth fold (CI < 0.2, Fig. 3C). The other two saponins B2 and F2a led to the same effect, therefore the further experiments were continued with B2 only. Based on the well-studied mode of action of ETP that it can induce apoptosis via both intrinsic and extrinsic pathways (Montecucco et al., 2015) and generate ROS (Shin et al., 2016) as a consequence of the inhibition of topoisomerase II and the accumulation of DNA breaks, we assessed the ability of the synergistic combinations of ETP with B2 or D2 to induce apoptosis and ROS in the treated cells at higher extend than the single application of ETP. First, the amount of generated intracellular ROS was measured as one of the characteristics of the mechanism of action of ETP. When the cells were treated with combinations between ETP and saponins B2 or D2 (20 µg/mL), significant difference between combined and single application was observed at concentrations equal or higher than 44.18 µg/ml ETP (Fig. 4A and Table S4). Thus, both saponins enhanced the cytotoxic potential of ETP as far as generation of ROS is related to increased DNA damage and cytotoxicity (Shin et al., 2016). As a next step we proved induction of apoptosis by three different methods: (1) caspases activation; (2) accumulation of mono- and oligonucleosomes levels in the cell cytosol and (3) DNA fragmentation. The results obtained from the caspase activation test confirmed the trend observed by the generation of ROS. Co-treatment with B2 or D2 significantly increased the pro-apoptotic potential of ETP at lower concentrations (44.18 µg/mL) than single ETP application

(176.7 µg/mL) for this cell line. In addition, markedly elevated mono- and oligonucleosomes levels were detected at 22.02 µg/mL ETP after co-treatment with 20 µg/mL B2 or D2 in difference to ETP alone, which is consistent with the observed high effect (Fa) of these combinations on cell viability. To further verify the synergistic effect of the aforementioned combinations, the changes of nuclear morphology in the treated cells were investigated by Hoechst 33342 DNA staining. The combination treatment of the cells led to apoptosis induction as witnessed by the observed nuclear fragmentation (Fig. 4D). Our results for the potential of saponins B2 and D2 to enhance cytotoxicity in combination with cytostatics are in line with other published data (Bottger et al., 2013; Li et al., 2014; Koczurkiewicz et al., 2016). Based on these results, we could conclude that saponin D2 was the most potent cytotoxicity enhancer which itself lacked *in vitro* cytotoxicity by the concentration used for the combinations (20 µg/ml).

In this study, we aimed also to bring an insight into the structure-activity relationship of tested saponins. An oleanane-type sapogenin (gypsogenin), a branched C-3 trisaccharide containing a xylose moiety and a C-28 ester-bonded oligosaccharide including the deoxy-sugars rhamnose and fucose together with an acetyl group attached to the glucose residue were mentioned as structure features for the synergistic cytotoxicity of *Gypsophila* GOTCABs with RIP I (Gevrenova et al., 2015). Branched C-3 and C-28 oligosaccharides occur in all tested saponins. Consequently, the impact of the remaining structural features such the presence of sulfate, acetyl and methoxycinnamoyl group(s), as well as the pentose residue in C-3, should be evaluated.

A distinct impact of sulfate group could be observed. Considerable differences in terms of effect Fa and CI were found between D2 and D1 (without sulfate group) and A2 and A1 (with sulfate group). The sulfate group was absent in all highly active enhancers, notably D2 and B2. Thus,

the combined effect of A1 with low concentrations of ETP was antagonistic, while synergism was achieved with high concentrations of ETP (CI 0.33 and 0.80) after 72 h of treatment. The combination treatment with A2 and the lowest and the highest concentrations of ETP showed synergistic effect (CI 0.62 and 0.81) (Table 2).

The substitution at the C-28 ester-bonded chain with acetyl group(s), being described previously for RIP I enhancers (Gevrenova et al., 2015), highly influenced the Fa and CI. Acetylation at Fuc C-4 is an advantageous feature for the strong synergistic effects of ETP and D2 in all tested combinations (Fig. 3). A further acetylation at Glc C-6 (B2) decreased the effect, as can be seen from CI values (CI=0.32, 22.02 µg/mL ETP + 20 µg/mL B2). (Fig. 3). The pentose moiety at the C-3 trisaccharide appeared the most significant factor. Saponins with arabinose (B2, D2) achieved higher efficiencies than those with a xylose residue (Table 2). An arabinose replaced by a xylose (D1, B1) led to distinctive effect decrease by lower concentrations of ETP (CI from 1.49 up to 4.57 for B1 combination) (Table 2). The substitution at the Fuc C-4 with *trans*-methoxycinnamoyl group also influenced the combined efficiency resulting in synergistic effect (Fig. 3 and Table 2).

In summary, a total of 28 GOTCABs together with 6 monodesmosides were identified or tentatively elucidated in *G. trichotoma* roots, including 21 pairs of isobars and 6 saponins undescribed in the literature. The present study is the first report on the synergistic effects of ETP with *G. trichotoma* GOTCABs towards Hodgkin lymphoma cells. The most potent enhancer was gypsogenin-based bidesmoside acetylated at Fuc C-4 in the ester-bonded chain. The mechanism of action could be through the activation of apoptosis witnessed by caspases activation, increased cellular mono-and oligonucleosomes levels and significant nuclear fragmentation. Furthermore, the combined treatment caused significant increase of ROS

generation. However, further investigation on the detailed molecular mechanisms is needed. *Gypsophila* GOTCABs might be considered as a promising adjuvant for lymphoma chemotherapy.

Acknowledgements: This study is financially supported by Project Д-76/03.05.2018, Council of Medical Science at Medical University - Sofia, Bulgaria. We thank Andrea Balukova (student, Bioprocessing of New Medicines, Department of Biochemical Engineering, UCL) for her devoted work on the *in vitro* cytotoxicity tests performed in the framework of her student's summer praxis. The fluorimetric measurements were performed with the kind support of Prof. Galya Staneva at the Institute of Biophysics and Biomedical Engineering, Bulgarian Academy of Sciences.

References

Allen, P. B., Leo I Gordon, L., 2017. Frontline therapy for classical hodgkin lymphoma by stage and prognostic factors. Clin. Med. Insights Oncol. 11, 1179554917731072.

Arslan, I., Celik, A., Melzig, M.F., 2013. Nebulosides A–B, novel triterpene saponins from under-ground parts of *Gypsophila arrostii* Guss. var. *nebulosa*. Bioorg. Med. Chem. 21, 1279-1283.

Bachran, C., Bachran, S., Sutherland, M., Bachran, D., Fuchs, H., 2008. Saponins in tumor therapy. Mini Rev Med Chem. 8, 575-584.

Bachran, C., Durkop, H., Sutherland, M., Bachran, D., Muller, C., Weng, A., Melzig, M.F., Fuchs, H., 2009. Inhibition of tumor growth by targeted toxins in mice is massively improved by Saponinum albumin a synergistic way. J. Immunother. 32, 713-725.

Biological evaluation of medical devices - Part 5: Tests for in vitro cytotoxicity, ISO 10993-5:2009, 2017. https://www.iso.org/standard/36406.html, International Organization for Standardization.

Bottger, S., Melzig, M. F., 2010. Triterpenoid saponins of the Caryophyllaceae and Illecebraceae family. Phytochem. Lett. 4, 59-68.

Bottger, S., Westhof, E., Siems, K., Melzig, M. F., 2013. Structure-activityrelationships of saponins enhancing the cytotoxicity of ribosome inactivating proteins type I (RIP-I). Toxicon 73, 144-150.

Chazotte, B., 2016. Labeling nuclear DNA with Hoechst 33342, Cold Spring Harb Protoc; doi:10.1101/pdb.prot087205.

Cheikh-Ali, S., Farman, M., Lacaille-Dubois, M.-A., Semma, N., 2019. Structural organization of saponins in Caryophyllaceae. Phytochem Rev. 18, 405-441.

Chen, Q., Luo, J. G., Kong, L. Y., 2011. New triterpenoid saponins from the roots of *Gypsophila perfoliata* Linn. Carbohydr. Res. 346, 2206-2212.

Chou, T. C., 1976. Derivation and properties of Michaelis-Menten type and Hill type equations for reference ligands. J. Theor. Biol. 59, 253-276.

Chou, T. C., 2006. Theoretical Basis, Experimental Design, and Computerized Simulation of Synergism and Antagonism in Drug Combination Studies. Pharmacol. Rev. 58, 621–681.

Chou, T. C., Martin, N., Eds., 2005. CompuSyn for drug combinations: PC software and user's guide: A computer program for quantitation of synergism and antagonism in drug combinations, and the determination of IC50 and ED50 and LD50 values. Paramus, (NJ), ComboSyn Inc.

Colleoni, G. W., Capodieci, P., Tickoo, S., Cossman, F., Filippa, D. A., Ladanyi, M., 2002. Expression of SSX genes in the neoplastic cells of Hodgkin's lymphoma. Hum. Pathol. 33, 496-502.

Devin, J., Lin, Y.-L., Kassambara, A., Cartron, G., Elemento, O., Constantinou, A., Pasero, Ph., Bret, C., Moreaux, J., 2017. Targeting DNA Repair Mechanisms to Overcome Drug Resistance in Diffuse Large B Cell Lymphoma. Blood 130 (Suppl 1), 1479-1479.

Diaz, T., Navarro, A., Ferrer, G., Gel, B., Gaya, A., Artells, R., Bellosillo, B., Garcia-Garcia, M., Serrano, S., Martinez, A., Monzo, M., 2011. Lestaurtinib inhibition of the Jak/STAT signaling pathway in hodgkin lymphoma inhibits proliferation and induces apoptosis. PloS one 6, e18856-e18856.

Du, G. J., Wang, C. Z., Zhang, Z. Y., Wen, X. D., Somogyi, J., Calway, T., He, T. C., Du, W., Yuan, C. S., 2012. Caspase-mediated pro-apoptotic interaction of panaxadiol and irinotecan in human colorectal cancer cells. J. Pharm. Pharmacol. 64, 727–734.

Frechet, D., Christ, B., Monegier du Sorbier, B., Fisher, H., Vuilhorgne, M., 1991. Four triterpenoid saponins from dried roots of *Gypsophil*a species. Phytochemistry 30, 927-931.

Fuchs, H., Bachran, D., Panjideh, H., Schellmann, N., Weng, A., Melzig, M. F., Sutherland, M., Bachran, C., 2009. Saponins as tool for improved targeted tumor therapies. Curr. Drug Targets 10, 140-151.

Fuchs, H., Niesler, N., Trautner, A., Sama, S., Jerz, G., Panjideh, H., Weng, A., 2017. Glycosylated triterpenoids as endosomal escape enhancers in targeted tumor therapies. Biomedicines 5, 1-25.

Gauthier, C., Legault, J., Girard-Lalancette, K., Mshvildadze, V, Pichette, A., 2009. Haemolytic activity, cytotoxicity and membrane cell permeabilisation of semi-synthetic and natural lupine- and oleanane-type saponins. Bioorg. Med. Chem. 2009, 17, 2002-2008.

Gevrenova, R., Bardarov, V., Bardarov, K., Voutquenne-Nazabadioko, L., Henry, M., 2018a. Selective profiling of saponins from *Gypsophila trichotoma* Wend. by HILIC separation and HRMS detection. Phytochem. Anal. 29, 250-274.

Gevrenova, R., Bardarov, K., Bouguet-Bonnet, S., Voynikov, Y., Balabanova, V., Zheleva-Dimitrova, D., Henry, M., 2018b. A new liquid chromatography-high resolution Orbitrap mass spectrometry-based strategy to characterize Glucuronide Oleanane-type Triterpenoid Carboxylic Acid 3,28-Bidesmosides (GOTCAB) saponins. A case study of *Gypsophila glomerata* Pall ex M. B. (Caryophyllaceae). J. Pharm. Biomed. Anal. 159, 567-581.

Gevrenova, R., Doytchinova, I., Kolodziej, B., Henry, M., 2019. In-depth characterization of the GOTCAB saponins in seven cultivated *Gypsophila* L. species (Caryophyllaceae) by liquid chromatography coupled with quadrupole-Orbitrap mass spectrometer. Biochem. Syst. Ecol. 83, 91-102.

Gevrenova, R., Joubert, O., Mandova, Tsv., Zaiou, M., Chapleur, Y., Henry, M., 2014. Cytotoxic effects of four Caryophyllaceae species extracts on macrophages cell lines. Pharm. Biol. 52, 919-925.

Gevrenova, R., Voutquenne-Nazabadioko, L., Harakat, D., Prost, E., Henry, M., 2006. Complete ^{1}H and ^{13}C NMR assignments of saponins from roots of *Gypsophila trichotoma* Wend. Magn. Res. Chem. 44, 686-691.

Gevrenova, R., Weng, A., Voutquenne-Nazabadioko, L., Thakur, M., Doytchinova, I. 2015. QSAR study on saponins as cytotoxicity enhancers. Lett. Drug Des. Discov. 12, 166-171.

Gilabert-Oriol, R., Mergel, K., Thakur, M., Mallinckrodt, B., Melzig, M.F., Fuchs, H., Weng, A., 2013. Real-time analysis of membrane permeabilizing effects of oleanane saponins. Bioorg. Med. Chem. 21, 2387-2395.

Henry, M., 2005. Saponins and phylogeny: Example of the "Gypsogenin group" saponins. Phytochem. Rev. 4, 89-94.

Kapoor, V., Singla, S., 2015. Herb-drug interactions – an update on synergistic interactions. J. Alt. Med. Res. 1, 1-11.

Kim, S. M., Lee, S. Y., Cho, J. S., Son, S. M., Choi, S. S., Yun, Y. P., Yoo, H. S., Yoon do, Y., Oh, K. W., Han, S. B., Hong, J. T., 2010. Combination of ginsenoside Rg3 with docetaxel enhances the susceptibility of prostate cancer cells via inhibition of NF-κB. Eur. J. Pharmacol. 631, 1-9.

Koczurkiewicz, P., Czyz, J., Podolak, I., Wojcik, K., Galanty, A., Janeczko, Z., Michalik, M., 2015. Multidirectional effects of triterpene saponins on cancer cells – mini-review of *in vitro* studies. Acta Biochim. Pol. 62, 383-393.

Koczurkiewicz, P., Kowolik, E., Podolak, I., Wnuk, D., Piska, K., Labedz-Maslowska, A., Wojcik-Pszczola, K., Pekala, E., Czyz, J., Michalik, M., 2016. Syneristic cytotoxic and anti-invasive effects of mitoxantrone and triterpene saponins from *Lysimahia ciliata* on human prostate cancer cells. Planta Med. 82, 1546-1552.

Li, Q., Deng, L., Li, W., Koike, K., 2014. Cyclamin, a natural 13,28-epoxy triterpenoid saponin, synergistically enhances the cytotoxicity of chemotherapeutic drugs in human liver cancer cells but not non-neoplastic liver cells. Planta Med. 80, 409-414.

Luo, J.-G., Ma, L., Kong, L.-Y. 2008. New triterpenoid saponins with strong [alpha]-glucosidase inhibitory activity from the roots of *Gypsophila oldhamiana*. Bioorg. Med. Chem. 16, 2912–2920.

Montecucco, A., Zanetta, F., Giuseppe Biamonti, G., 2015. Molecular mechanisms of etoposide. EXCLI Journal 14, 95-108.

Mosmann, T. 1983. Rapid colorimetric assay for cellular growth and survival: application to proliferation and cytotoxicity assays. J. Immunol. Methods 65, 55-63.

Nie, W., Luo, J.-G., Wang, X. B., Kong, L.-Y. 2009. An insight into enrichment and separation of oleanane-type triterpenoid saponins by various chromatographic materials. Sep. Purif. Technol. 65, 243-247.

Nord, L.I., Kenne, L., 2000. Novel acetylated saponin in a chromatographic fraction from *Quillaja saponaria* Molina. Carbohydr. Res. 329, 817-829.

Pertuit, D., Avunduk, S., Mitaine-Offer, A.-C., Miyamoto, T., Tanaka, Ch., Paululat, Th., Delemasure, S., Dutartre, P., Lacaille-Dubois, M.-A., 2014. Triterpenoid saponins from the roots of two *Gypsophila* species, Phytochemistry 102, 182-188.

Sarkar, F. H, Li, Y., 2006. Using chemopreventive agents to enhance the efficacy of cancer therapy. Cancer Res. 66, 3347-3350.

Shin H. J., Kwon, H. K., Lee, J. H., Anwar, M. A., Choi, S., 2016. Etoposide induced cytotoxicity mediated by ROS and ERK in human kidney proximal tubule cells. Sci. Rep. 6, 34064.

Voutquenne-Nazabadioko, L., Gevrenova, R., Borie, N., Harakat, D., Sayagh, Ch., Weng, A., Thakur, M., Zaharieva, M., Henry, M., 2013. Triterpenoid saponins from the roots of *Gypsophila trichotoma* Wender. Phytochemistry 90, 114-127.

Wang, Q., Zheng, X. L., Yang, L., Shi, F., Gao, L. B., Zhong, Y. J., Sun, H., He, F., Lin, Y., Wang, X., 2010. Reactive oxygen species-mediated apoptosis contributes to chemosensitization effect of saikosaponins on cisplatin-induced cytotoxicity in cancer cells. J. Exp. Clin. Cancer Res. 29, 150–159.

Weng, A., Jenett-Siems, K., Schmieder, P., Bachran, D., Bachran, C., Gorick, C., Thakur, M., 2010. A convenient method for saponin isolation in tumour therapy. J. Chromatogr. B 878, 713-718.

Xu, X.-H., Li, T., Fong, C., Fong, C. M. V., Chen, X., Chen, X.-J., Wang, Y.-T., Huang, M.-Q., Lu, J.-J. 2016. Saponins from Chinese medicine as anticancer agents. Molecules 1326, 1-27.

Yao, S., Ma, L., Luo, J.-G., Wang, J.-S., Kong, L.-Y., 2010. New Triterpenoid Saponins from the Roots of *Gypsophila paniculata* L. Helv. Chim. Acta 93, 361-374.

Yotova, M., Krasteva, I., Jenett-Siems, K., Zdraveva, P., Nikolov, S. 2012. Triterpenoids in *Gypsophila trichotoma* Wend. Phytochem. Lett. 5, 752-755.

Zaharieva, M. M., Trochopoulos, A., Dimitrova, L., Berger, M. R., Najdenski, H., Konstantinov, S., Kroumov, A. D., 2018. New insights in routine procedure for mathematical evaluation of in vitro cytotoxicity data from cancer cell lines. Int. Journal Bioautomation 22, 87-106.

Zhang, Q., Kang, X., Yang, B., Wang, J., Yang, F., 2008. Antiangiogenic effect of capecitabine combined with ginsenoside Rg3 on breast cancer in mice. Cancer Biother. Radiopharm. 23, 647–653.

Zhang, W., Luo, J.-G., Zhang, C., Kong L.-Y., 2013. Different apoptotic effects of triterpenoid saponin-rich *Gypsophila oldhamiana* root extact on hamun hepatoma SMMC-7721 and normal hamun hepatic L02 cells. Biol. Pharm. Bull. 36, 1080-108.